Zero-Dimensional Organic-inorganic Hybrid Indium Halide Perovskite with Broadband Yellow Light Emission

Qi Wang,[ab] Wei Jiang,[a] Peng-Yao Xuan,[a] Ke Zhao,[a] Xiu-Yue Fu,[a] Xiao-Rui Zhang,[a] Xiao-Wu Lei,[a] Cheng-Yang Yue,[a*] Xiang-Wen Kong [a*]

[a] Research institute of Optoelectronic Functional Materials, School of Chemistry, Chemical Engineer and Materials, Jining University, Qufu, Shandong, 273155, P. R. China

[b] School of Chemistry and Chemical Engineering, Qufu Normal University, Qufu, Shandong, 273165, P. R. China

Corresponding Authors: Cheng-Yang Yue; Xiang-Wen Kong

E-mail: yuechengyang@126.com; kongxiangwen@jnxy.edu.cn

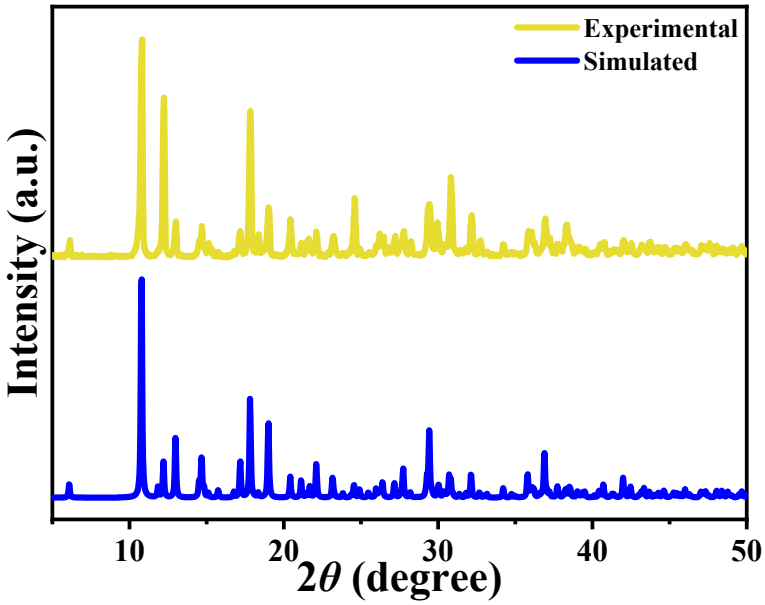

Figure S1. The simulated and experimental powder X-ray diffraction (PXRD) patterns of $[1\text{-Me-Pipz}]_2[InCl_6]Cl{\cdot}H_2O$.

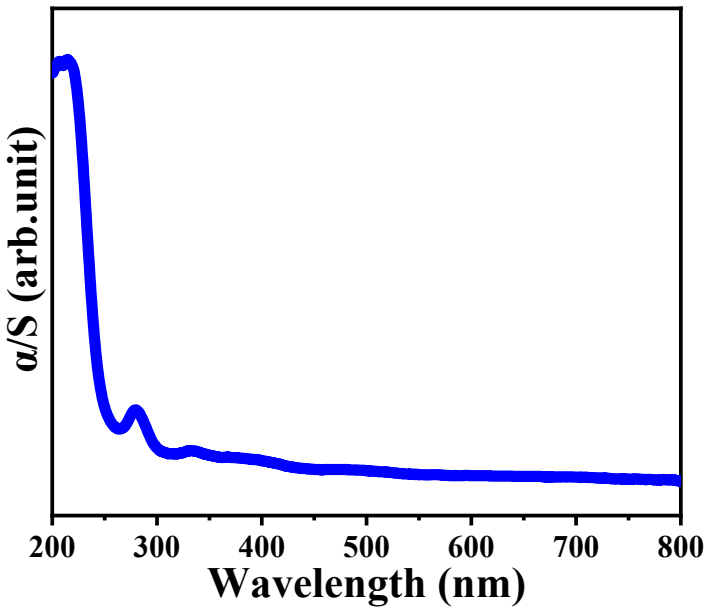

Figure S2. The UV-vis absorption spectrum of $[1\text{-Me-Pipz}]_2[InCl_6]Cl{\cdot}H_2O$.

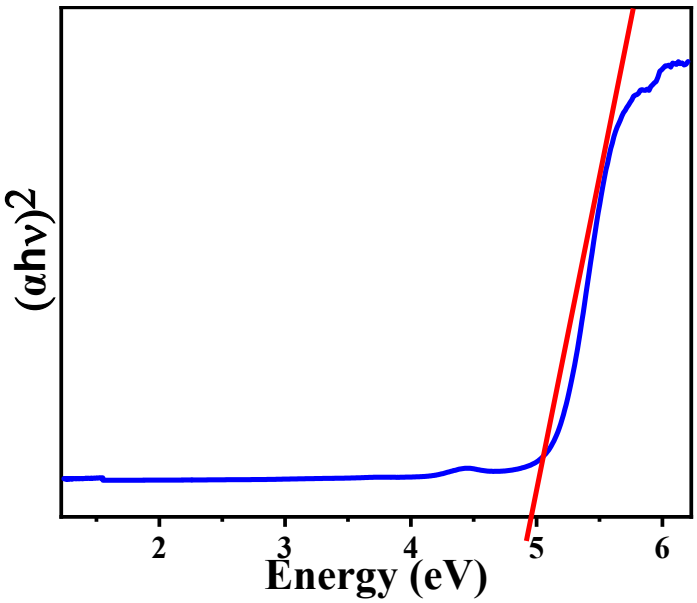

Figure S3. The Tauc's plot for $[1\text{-Me-Pipz}]_2[InCl_6]Cl{\cdot}H_2O$.

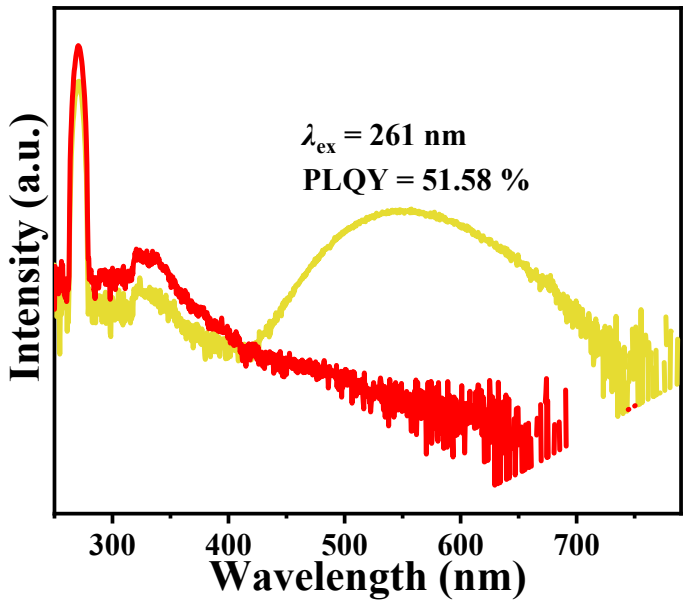

Figure S4. The PLQY of $[1\text{-Me-Pipz}]_2[InCl_6]Cl{\cdot}H_2O$ at 300K.

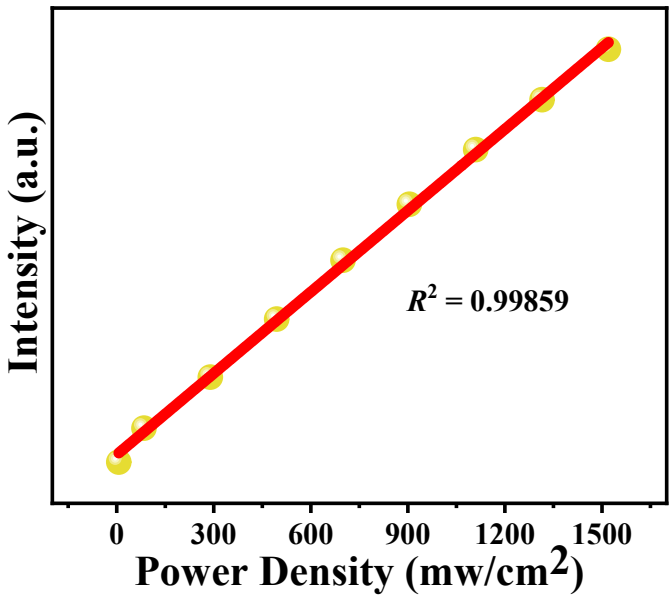

Figure S5. The PL emission of $[1\text{-Me-Pipz}]_2[InCl_6]Cl{\cdot}H_2O$ as a function of power density.

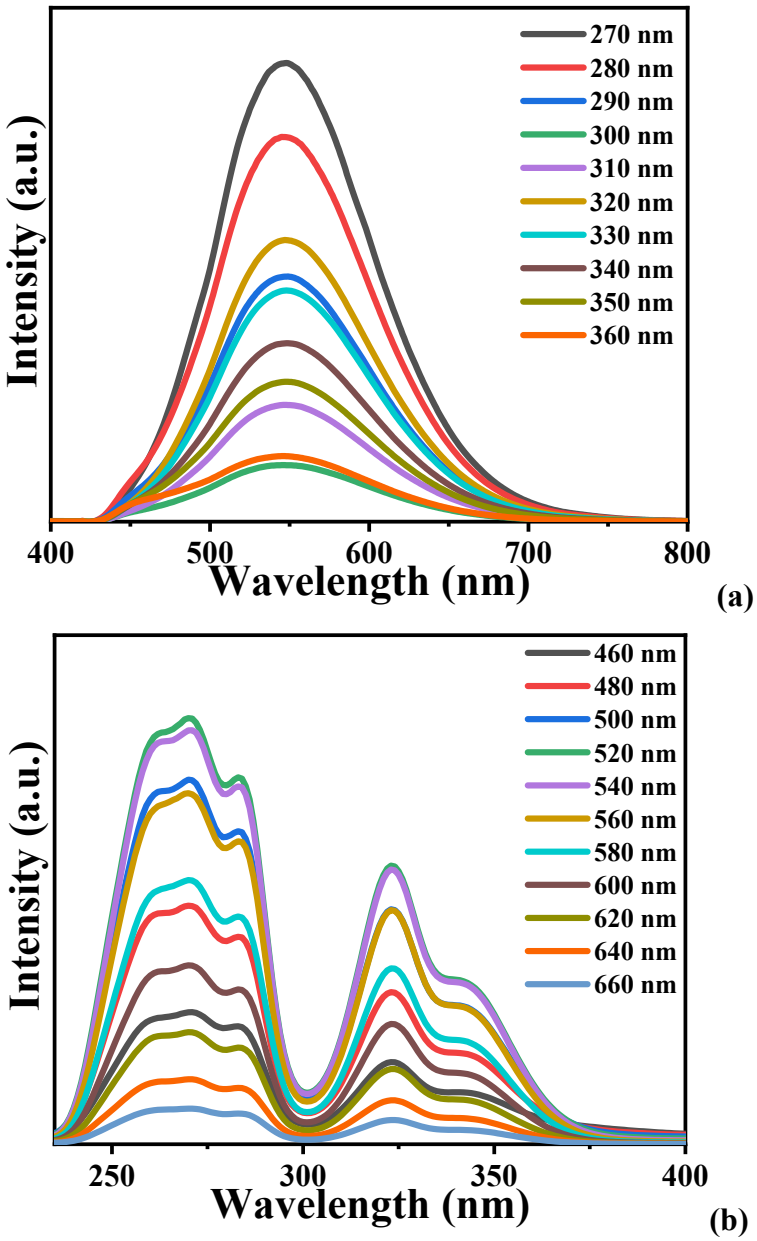

Figure S6. The excitation wavelength dependent PL emission spectra (a) and the emission wavelength dependent PL excitation spectra (b) of [1-Me-Pipz]$_2$[InCl$_6$]Cl·H$_2$O.

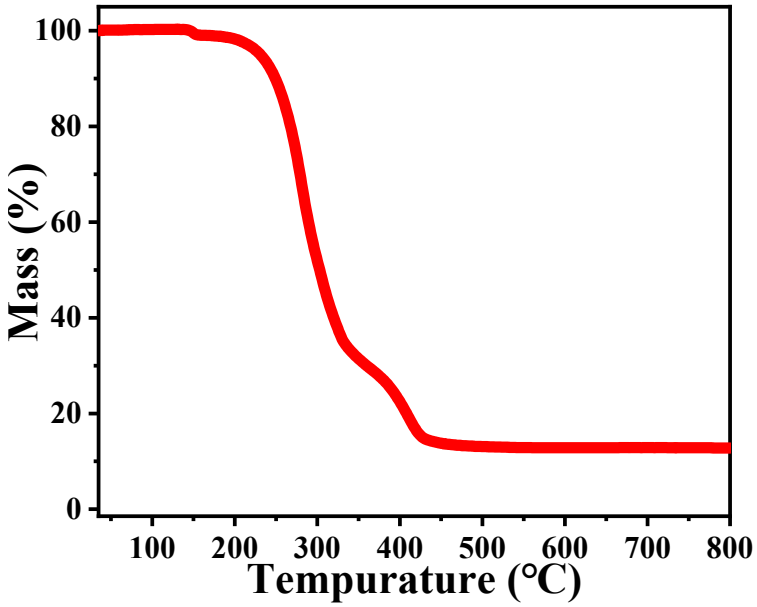

Figure S7. The thermogravimetric analysis of $[1\text{-Me-Pipz}]_2[InCl_6]Cl{\cdot}H_2O$.

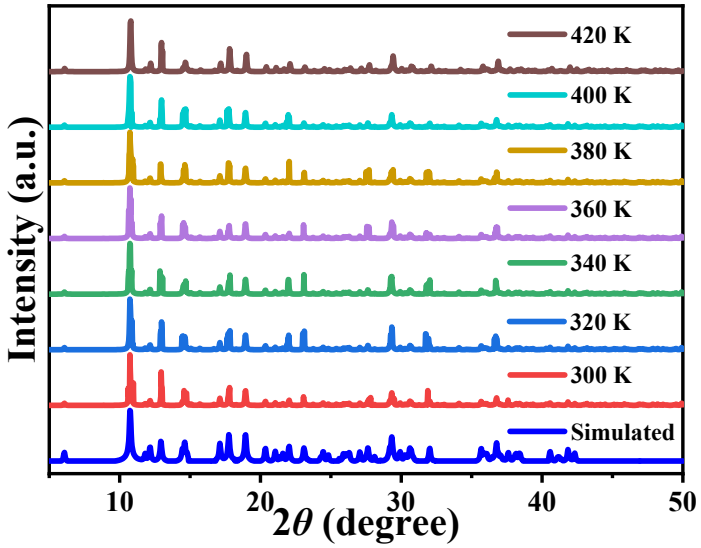

Figure S8. The simulated and experimental powder X-ray diffraction (PXRD) patterns of $[1\text{-Me-Pipz}]_2[InCl_6]Cl{\cdot}H_2O$ after continuous heating from 300 K to 420 K.

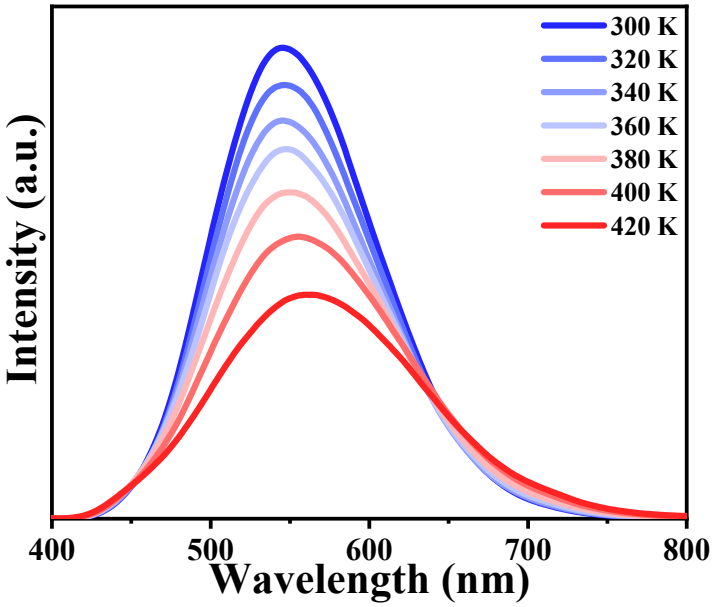

Figure S9. The PL emission spectra of $[1\text{-Me-Pipz}]_2[InCl_6]Cl{\cdot}H_2O$ after continuous heating from 300 K to 420 K.

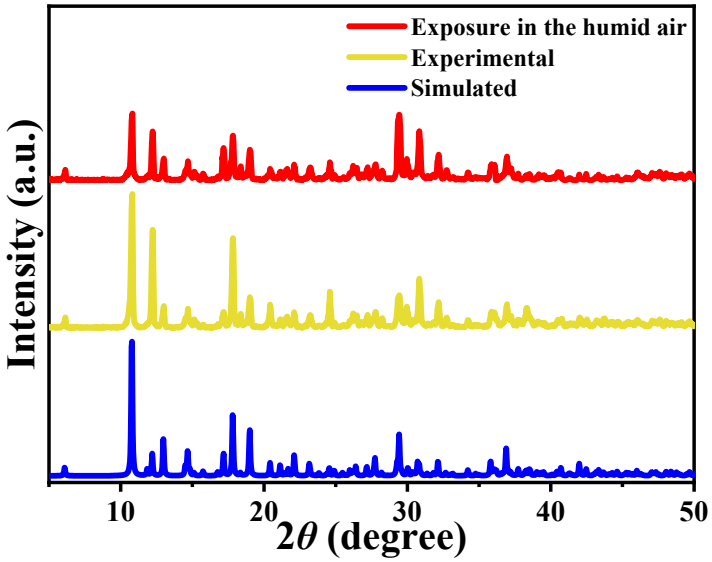

Figure S10. The simulated and experimental powder X-ray diffraction (PXRD) patterns of $[1\text{-Me-Pipz}]_2[InCl_6]Cl{\cdot}H_2O$ before and after storing in ambient atmosphere with relative humidity of about 50% for one week.

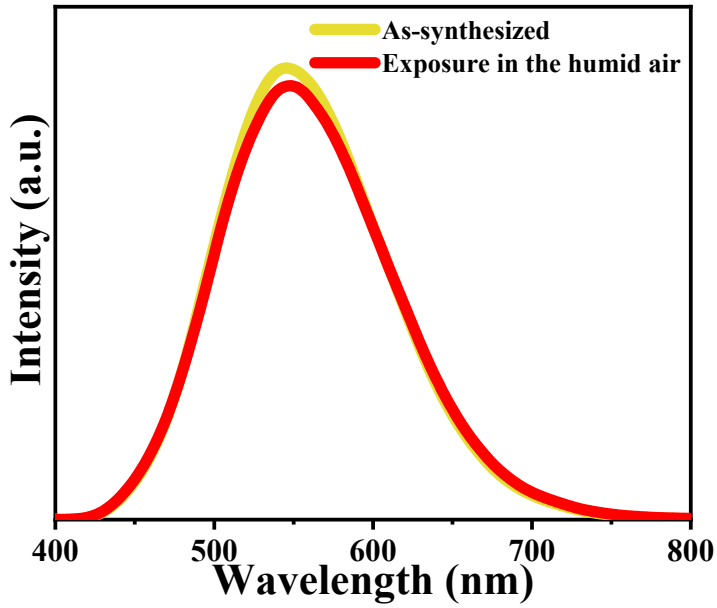

Figure S11. The PL spectra of $[1\text{-Me-Pipz}]_2[InCl_6]Cl{\cdot}H_2O$ before and after storing in ambient atmosphere with relative humidity of about 50% for one week.

Table S1. Crystal Data and Structural Refinements for $[1\text{-Me-Pipz}]_2[InCl_6]Cl\cdot H_2O$.

Compound	$[1\text{-Me-Pipz}]_2[InCl_6]Cl\cdot H_2O$
chemical formula	$C_{10}H_{30}Cl_7InN_4O$
fw	585.35
Space group	*Pnma*
a/Å	28.989(9)
b/Å	9.949(3)
c/Å	7.723(3)
α/°	90
β/°	90
γ/°	90
V(Å^3)	2227.4(13)
Dcalcd (g·cm^{-3})	1.746
Temp (K)	296.15
μ (mm^{-1})	1.907
F (000)	1176.0
Reflections collected	26057
Independent reflections	2964
GOF on F^2	1.017
[a]R_1, wR_2 ($I > 2\sigma(I)$)	0.0277/ 0.0586
[b]R_1, wR_2 (all data)	0.0378/ 0.0620

[a]$R_1 = \sum||F_o| - |F_c||/\sum|F_o|$. [b]$wR_2 = [\sum w(F_o^2 - F_c^2)^2/\sum w(F_o^2)^2]^{1/2}$.

Table S2. Selected bond lengths (Å) and bond angles (°) for compound [1-Me-Pipz]$_2$[InCl$_6$]Cl·H$_2$O.

In1-Cl1	2.5386(11)	In1-Cl3 #1	2.5102(9)
In1-Cl2	2.4910(11)	In1-Cl4	2.5166(9)
In1-Cl3	2.5102(9)	In1-Cl4 #1	2.5166(9)

Symmetry codes: #1: 1+*x*, 3/2-*y*, +*z*

Table S3. Hydrogen bonds data for [1-Me-Pipz]$_2$[InCl$_6$]Cl·H$_2$O.

D-H···A	d(D-H)	d(H···A)	d(D···A)	<(DHA)
N(1)-H(1A)···Cl(4)	0.89	2.63	3.351(3)	139
N(1)-H(1A)···Cl(4)	0.89	2.63	3.351(3)	139
N(1)-H(1B)···Cl(1)	0.89	2.62	3.246(3)	128
N(1)-H(1B)···Cl(3)	0.89	2.82	3.507(3)	135
N(1)-H(1B)···Cl(3)	0.89	2.82	3.507(3)	135
O(1)-H(1E)···Cl(5)	0.85	2.59	3.180(4)	127
O(1)-H(1E)···Cl(4)	0.85	2.72	3.3059(16)	127
O(1)-H(1F)···Cl(4)	0.85	2.71	3.3059(16)	128
N(2)-H(2)···O(1)	0.98	1.77	2.731(5)	165
N(3)-H(3)···Cl(5)	0.98	2.05	3.016(3)	171
N(4)-H(4A)···Cl(3)	0.89	2.61	3.330(3)	139
N(4)-H(4A)···Cl(3)	0.89	2.61	3.330(3)	139
N(4)-H(4B)···Cl(2)	0.89	2.68	3.276(3)	125
N(4)-H(4B)···Cl(4)	0.89	2.81	3.506(3)	136
N(4)-H(4B)···Cl(4)	0.89	2.81	3.506(3)	136
C(2)-H(2A)···Cl(3)	0.97	2.81	3.681(3)	149
C(3)-H(3A)···Cl(3)	0.96	2.70	3.544(2)	147
C(3)-H(3B)···Cl(3)	0.96	2.63	3.544(2)	159